Supporting Information

Photon Upconversion in Yb^{3+}–Tb^{3+} and Yb^{3+}–Eu^{3+} Activated Core/Shell Nanoparticles with Dual-Band Excitation

Hao Dong,[a] Ling-Dong Sun,[a] Ye-Fu Wang,[a] Jia-Wen Xiao,[a] Datao Tu,[b] Xueyuan Chen,[b] Chun-Hua Yan*[a]*

[a] Beijing National Laboratory for Molecular Sciences, State Key Laboratory of Rare Earth Materials Chemistry and Applications, PKU-HKU Joint Laboratory in Rare Earth Materials and Bioinorganic Chemistry, College of Chemistry and Molecular Engineering, Peking University, Beijing 100871, China.

[b] Key Laboratory of Optoelectronic Materials Chemistry and Physics, Fujian Institute of Research on the Structure of Matter, Chinese Academy of Sciences, Fuzhou, Fujian 350002, China.

E-mail: sun@pku.edu.cn; yan@pku.edu.cn

Experimental Section

Preparation of $RE(CF_3COO)_3$: In a typical procedure, rare earth oxides were added to a solution containing excess amount of trifluoroacetic acid with strong stirring and heating. The reaction stopped when a transparent solution formed. The resulting solution was then filtered to remove insoluble impurities. Finally, the following solution was concentrated and dried at 140 °C to make $RE(CF_3COO)_3$ powders.

Synthesis of hexagonal phased $NaGdF_4$:Yb,A,Tm@$NaGdF_4$:Nd,Yb Nanoparticles (A = Tb, Eu): The synthetic procedures of hexagonal phased $NaGdF_4$:Yb,A,Tm@$NaGdF_4$:Nd,Yb nanoparticles were similar with that of $NaGdF_4$:Yb,A@$NaGdF_4$:Nd,Yb nanoparticles, except the additional dosage of $Tm(CF_3COO)_3$.[S1]

Synthesis of hexagonal phased $NaGdF_4$:Yb,A@$NaGdF_4$:Yb,Tm@$NaYF_4$:Nd,Yb Nanoparticles (A = Tb, Eu): The hexagonal phased $NaGdF_4$:Yb,A@$NaGdF_4$:Yb,Tm nanoparticles were similar with that of $NaGdF_4$:Yb,A@$NaGdF_4$:Nd,Yb nanoparticles. The outer shell layer was introduced as follows. 2.5 mL as-prepared hexagonal phased $NaGdF_4$:Yb,A@$NaGdF_4$:Yb,Tm core/shell colloidal solutions were redispersed in 40 mmol OA, ODE mixture (molar ratio 1:1), and an extra $RE(CF_3COO)_3$ (RE = Y, Nd, Yb, 1 mmol) and CF_3COONa (1 mmol) were added. Then the slurry was heated to 110 °C to remove cyclohexane, water and oxygen with vigorous magnetic stirring under vacuum, and formed a clear solution. The solution was heated to 310 °C and kept for 30 min under N_2 atmosphere. Upon cooling to room temperature, the hexagonal phased $NaGdF_4$:Yb,A@$NaGdF_4$:Yb,Tm@$NaYF_4$:Nd,Yb nanoparticles were collected by centrifugation after adding excess amount of ethanol. Finally, the product was dispersed in 5 mL of cyclohexane.

In vivo Imaging

In vivo imaging experiments were performed with a CALIPER Lumina II *in vivo* imaging system (IVIS). BALB/c nude mice were anesthetized by injecting chloral hydrate (5% aqueous solution, 100 μL) and then immobilized on the imaging stage of IVIS. White-light images and luminescence images were captured individually with the exposure time of 0.1 s and 1.0 s, respectively. The excitation power densities for both lasers were tuned to 500 mW cm^{-2}. A 680-sp filter, a 535/150+680sp filter (green), and a 625/90+680sp (red) filter were used as emission filters for *in vivo* imaging tests under both 980 nm and 808 nm excitations. All the animal experiments were performed in agreement with the guidelines of Beijing Association on Laboratory Animal Care and performed in accordance with institutional guidelines on animal handling.

Table S1. ICP-AES analyses of typical as-prepared nanoparticles.

Nominal	$NaGdF_4$:20%Yb,5%Tb	$NaGdF_4$:20%Yb,10%Tb
ICP-AES result	$NaGdF_4$:14.9%Yb,3.5%Tb	$NaGdF_4$:18.1%Yb,8.9%Tb
Nominal	$NaGdF_4$:80%Yb,10%Tb	$NaGdF_4$:20%Yb,10%Tb@$NaGdF_4$:50%Nd,10% Yb
ICP-AES result	$NaGdF_4$:74.9%Yb,10.6%Tb	$NaGdF_4$:18.1%Yb,8.9%Tb@$NaGdF_4$:49.6%Nd, 5.6%Yb

It can be found that the resulting doping concentrations of $Yb^{3+}/Tb^{3+}/Nd^{3+}$ acquired from ICP-AES analyses are similar to the nominal ones.

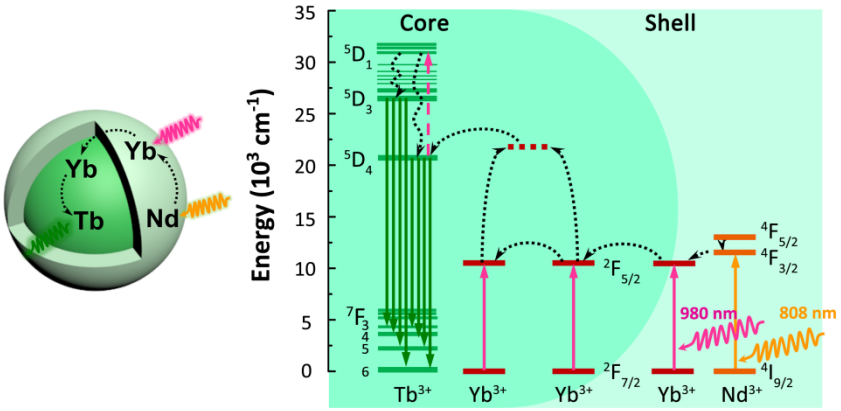

Scheme S1. Schematic design (left) and simplified energy transfer diagram of $NaGdF_4$:Yb,Tb@$NaGdF_4$:Nd,Yb nanoparticle under NIR excitation (right). Note that only partial energy levels of Nd^{3+} and Tb^{3+} are shown for clarity.

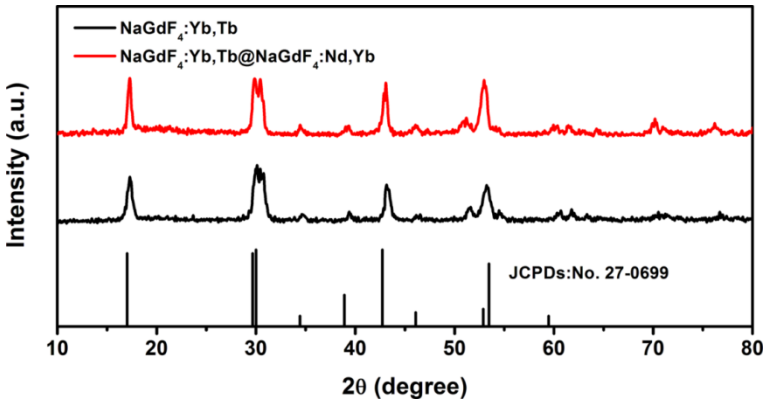

Figure S1. XRD patterns of $NaGdF_4$:30%Yb,10%Tb and $NaGdF_4$:30%Yb,10%Tb@$NaGdF_4$:50%Nd,10%Yb nanoparticles. Both of them can be assigned to hexagonal phased structure.

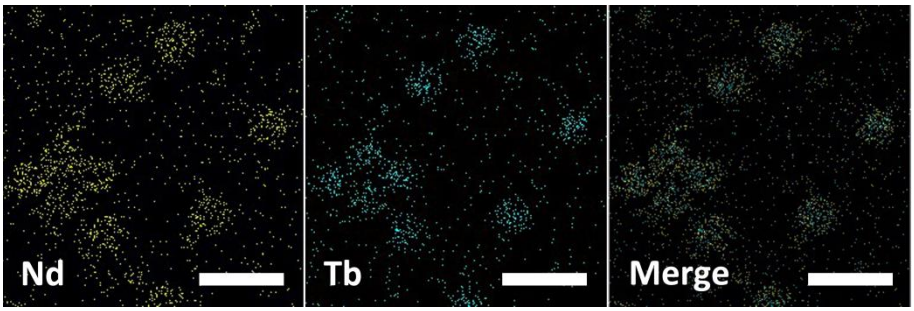

Figure S2. EDX-mapping images of $NaGdF_4$:20%Yb,10%Tb@$NaGdF_4$:50%Nd,10%Yb nanoparticles. It can be found that Nd^{3+} ions are distributed in the outer shell, while Tb^{3+} ions locate in inner core region. Scale bars are 50 nm.

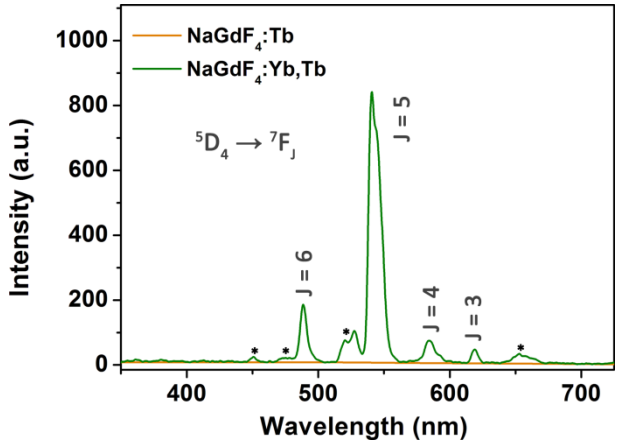

Figure S3. Upconversion emission spectra of $NaGdF_4$:10%Tb and $NaGdF_4$:30%Yb,10%Tb nanoparticles under 980 nm excitation. Note that emissions of the impurity (Tm^{3+} and Er^{3+}) are marked with "*".

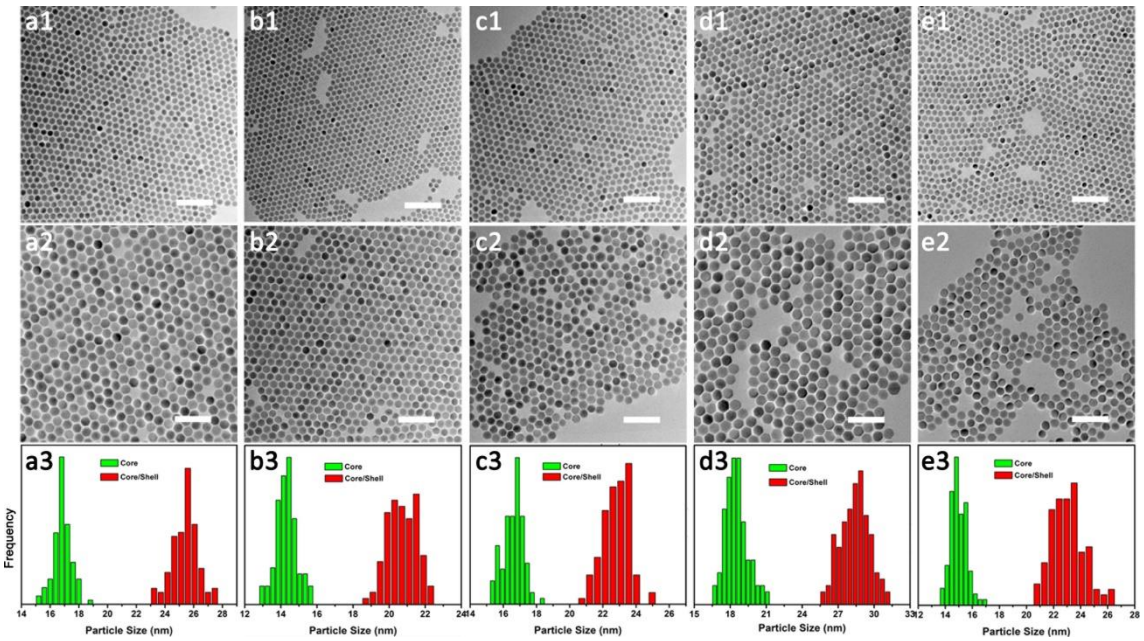

Figure S4. TEM images of $NaGdF_4$:20%Yb,Tb (a1 – e1), $NaGdF_4$:20%Yb,Tb@$NaGdF_4$:50%Nd,10%Yb (a2 – e2), and corresponding size distributions (a3 – e3) with different Tb^{3+} doping concentration in the core. a, 0.2%; b, 1%; c, 5%; d, 10%; e, 20%. Scale bars are 100 nm.

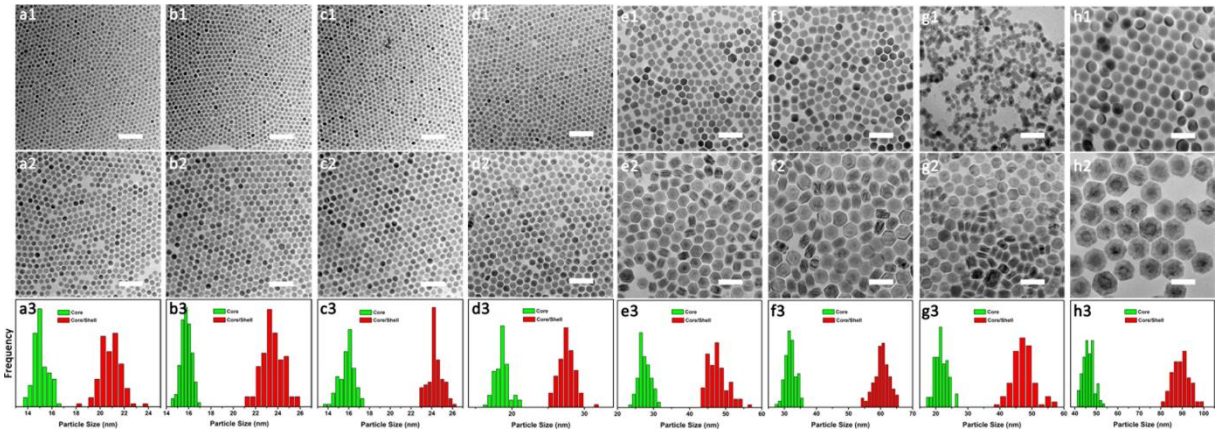

Figure S5. TEM images of $NaGdF_4$:Yb,10%Tb (a1 – h1), $NaGdF_4$:Yb,10%Tb@$NaGdF_4$:50%Nd,10%Yb (a2 – h2), and corresponding size distributions (a3 – h3) with different Yb^{3+} doping concentration in the core. a, 10%; b, 30%; c, 40%; d, 50%; e, 60%; f, 70%; g, 80%; h, 90%. Scale bars are 100 nm. It can be found that particle sizes of nanoparticles with high content of Yb^{3+}, typically more than 50%, are larger than those of nanoparticles with less content of Yb^{3+}. This is due to that $NaYbF_4$ is more stabilized in cubic phase, and needs more energy to process the phase transition to hexagonal phase. This has also been discovered in previous studies.[S1a]

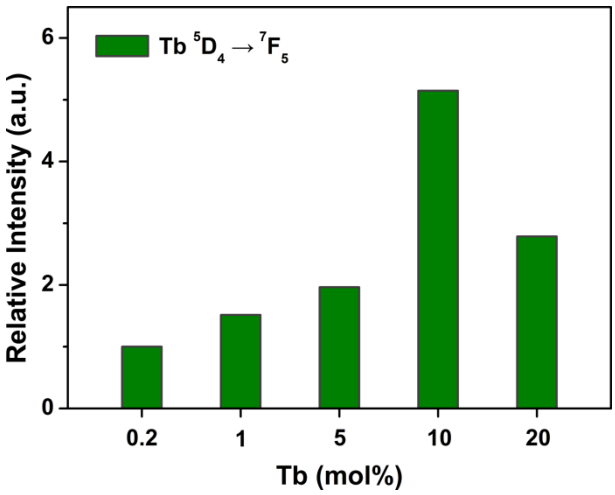

Figure S6. Relative intensity of Tb^{3+} emission as a function of the doping concentration of Tb^{3+}.

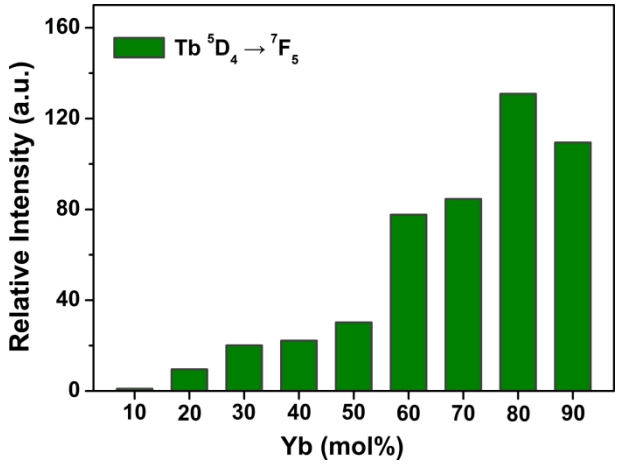

Figure S7. Relative intensity of Tb^{3+} emission as a function of the doping concentration of Yb^{3+}.

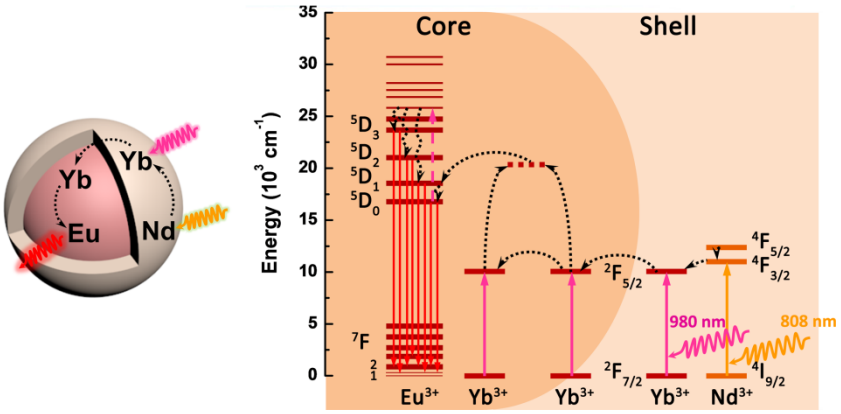

Scheme S2. Schematic design (left) and simplified energy transfer diagram of $NaGdF_4$:Yb,Eu@$NaGdF_4$:Nd,Yb nanoparticle under NIR excitation (right). Note that only partial energy levels of Nd^{3+} and Eu^{3+} are shown for clarity.

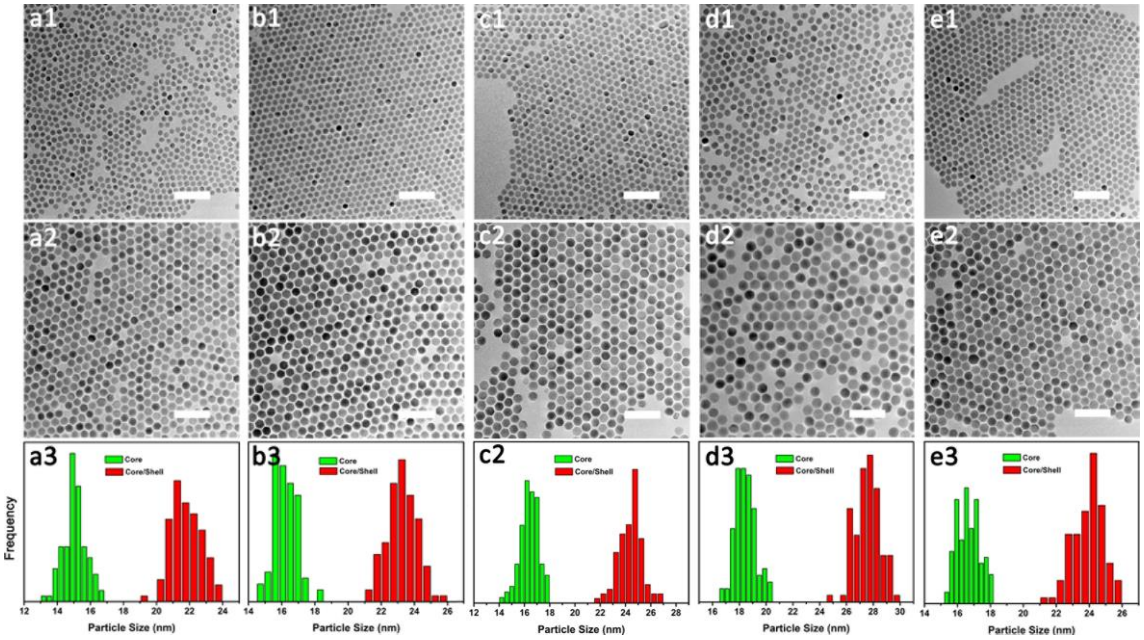

Figure S8. TEM images of $NaGdF_4$:20%Yb,Eu (a1 – e1), $NaGdF_4$:20%Yb,Eu@$NaGdF_4$:50%Nd,10%Yb (a2 – e2), and corresponding size distributions (a3 – e3) with different Eu^{3+} doping concentration in the core. a, 0.2%; b, 1%; c, 5%; d, 10%; e, 20%. Scale bars are 100 nm.

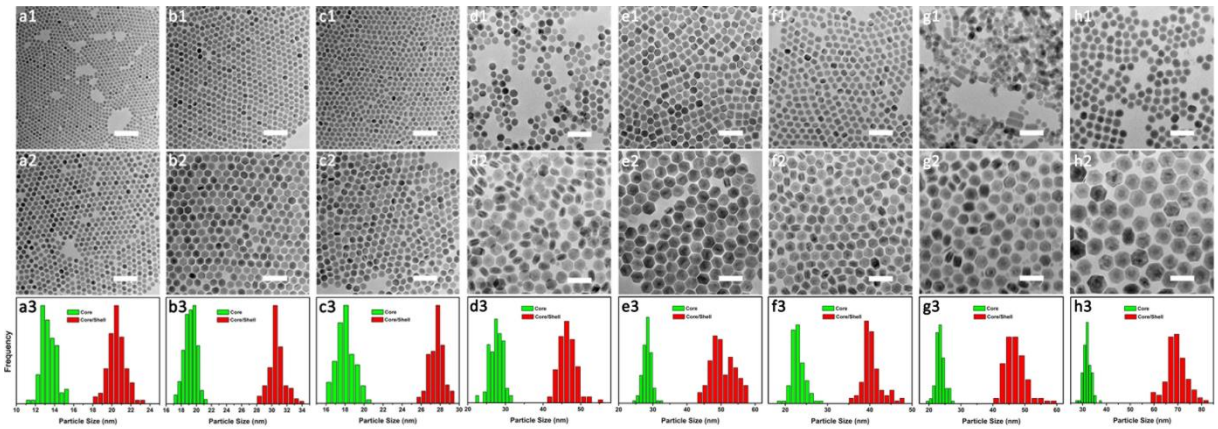

Figure S9. TEM images of $NaGdF_4$:Yb,10%Eu (a1 – h1), $NaGdF_4$:Yb,10%Eu@$NaGdF_4$:50%Nd,10%Yb (a2 – h2), and corresponding size distributions (a3 – h3) with different Yb^{3+} doping concentration in the core. a, 10%; b, 30%; c, 40%; d, 50%; e, 60%; f, 70%; g, 80%; h, 90%. Scale bars are 100 nm.

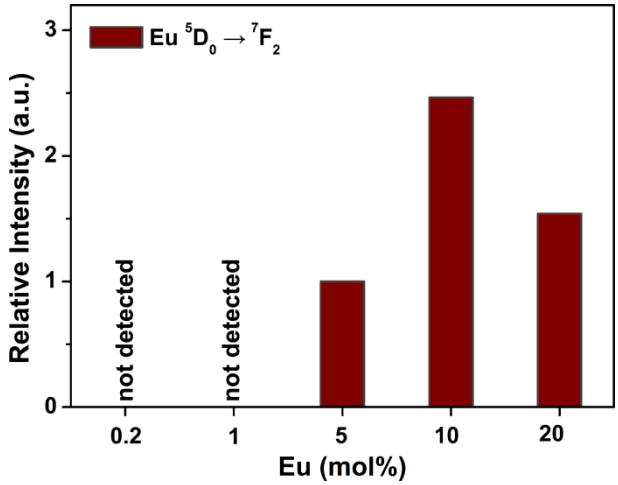

Figure S10. Relative intensity of Eu^{3+} emission as a function of the doping concentration of Eu^{3+}.

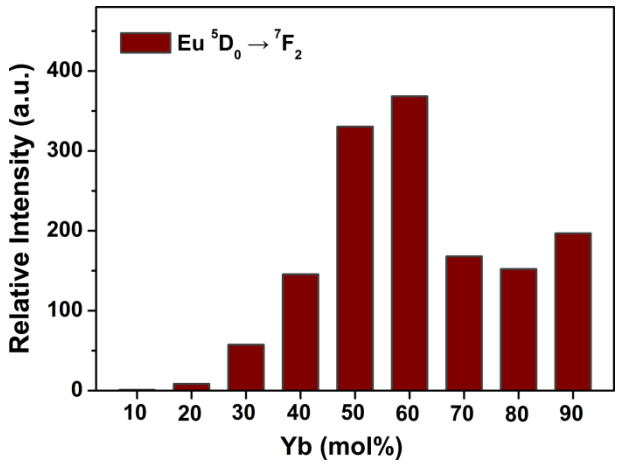

Figure S11. Relative intensity of Eu^{3+} emission as a function of the doping concentration of Yb^{3+}.

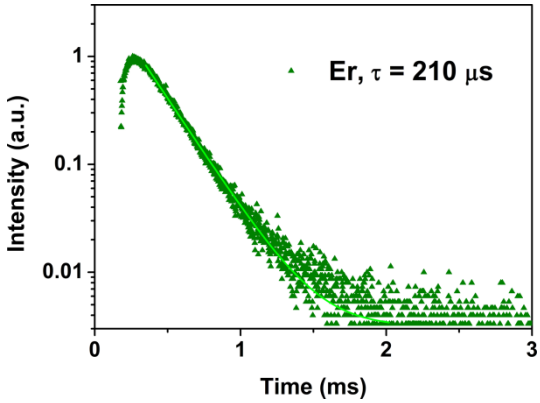

Figure S12. Upconversion emission lifetimes of Er^{3+} (λ_{em} = 542 nm) activated nanoparticles under 980 nm excitation. It can be found that emission lifetimes of Er^{3+} is much shorter than the millisecond lifetimes of Tb^{3+} and Eu^{3+}.

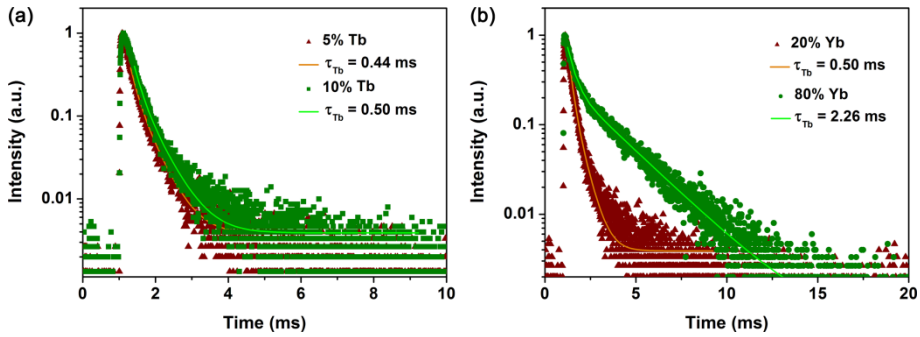

Figure S13. The content of Tb^{3+} (a) and Yb^{3+} (b) dependent upconversion emission decay curves of green emission at 542 nm in $NaGdF_4$:20%Yb,*x*Tb@$NaGdF_4$:50%Nd,10%Yb (*x* = 5%, 10%) (a) and $NaGdF_4$:*x*%Yb,10%Tb@$NaGdF_4$:50%Nd,10%Yb (*x* = 20, 80%) (b).

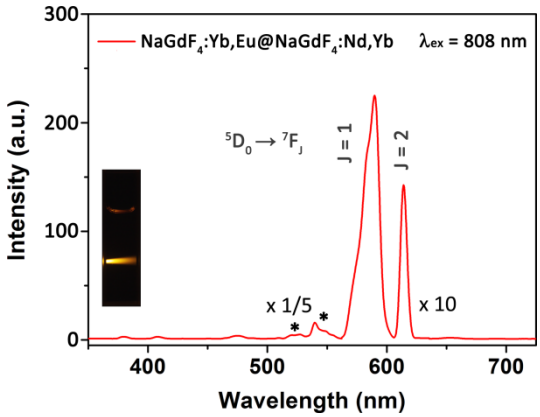

Figure S14. Upconversion emission spectra of $NaGdF_4$:30%Yb,10%Eu@$NaGdF_4$:50%Nd,10%Yb nanoparticles under 808 nm excitation. Note that emissions of the impurity (Tm^{3+} and Er^{3+}) are marked with "*".

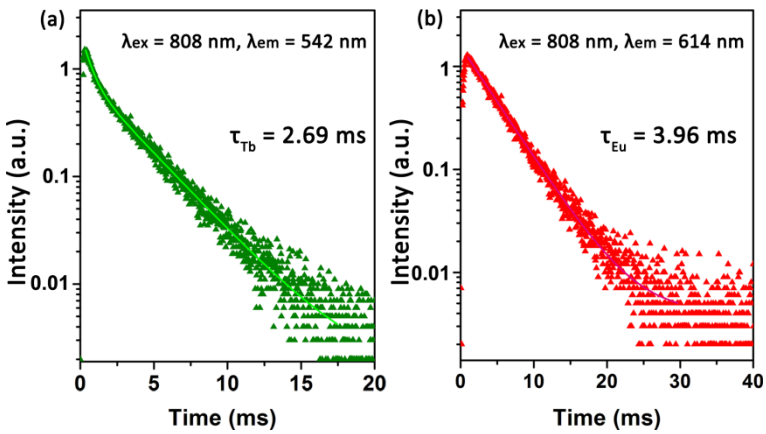

Figure S15. Upconversion decay curves of $NaGdF_4$:30%Yb,10%A@$NaGdF_4$:50%Nd,10%Yb (A = Tb (a), Eu (b)) nanoparticles under 808 nm excitation, respectively. Insets are fitted lifetimes.

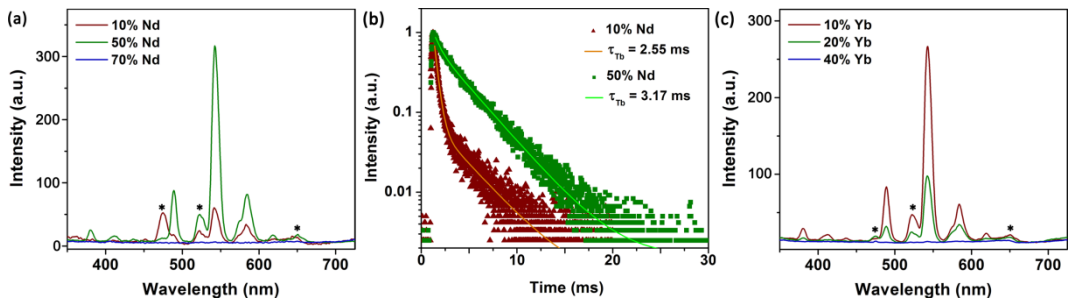

Figure S16. Upconversion emission spectra of $NaGdF_4$:40%Yb,10%Tb@$NaGdF_4$:Nd,Yb nanoparticles as a function of Nd^{3+} (a) and Yb^{3+} (c) content under 808 nm excitation. Note that upconversion emissions of the impurity (Tm^{3+} and Er^{3+}) are marked with "*". (b) Green emission decay curves of $NaGdF_4$:40%Yb,10%Tb@$NaGdF_4$:*x*Nd,10%Yb (*x* = 10%, 50%) nanoparticles.

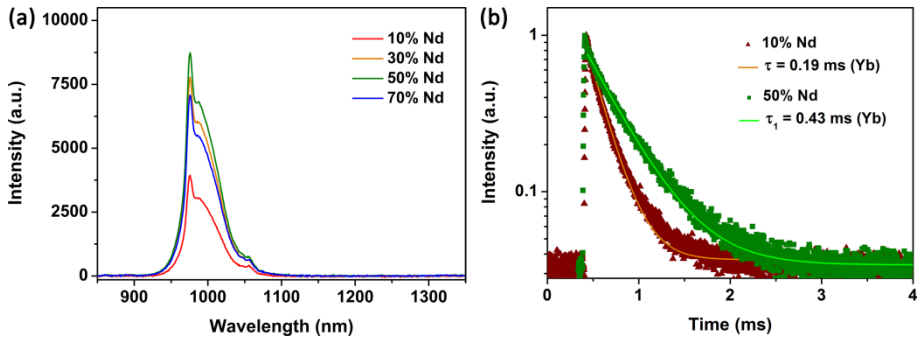

Figure S17. Near-Infrared emission spectra and corresponding emission decay curves (λ_{em} = 1000 nm) of $NaGdF_4$:40%Yb,10%Tb@$NaGdF_4$:Nd,Yb nanoparticles as a function of Nd^{3+} (a) content under 808 nm excitation. It can be found that 50% Nd^{3+} are more suitable in shell.

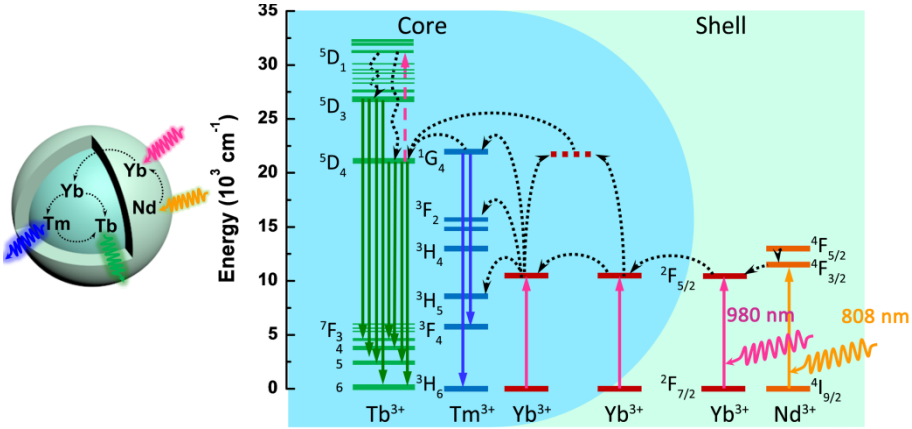

Scheme S3. Schematic design (left) and simplified energy transfer diagram of multicolor-emitting $NaGdF_4$:Yb,Tb,Tm@$NaGdF_4$:Nd,Yb nanoparticles under NIR excitation. Note that only partial energy levels of Nd^{3+}, Tb^{3+} and Tm^{3+} are shown for clarity.

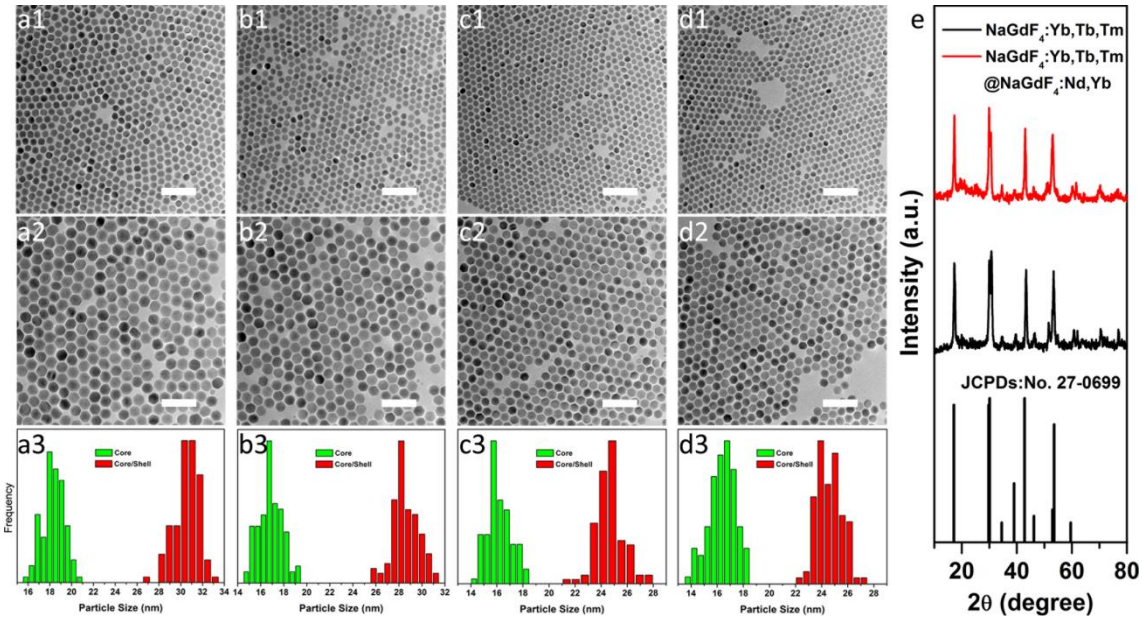

Figure S18. (a – d) TEM images of $NaGdF_4$:30%Yb,10%Tb,Tm (a1 – d1), $NaGdF_4$:30%Yb,10%Tb,Tm@$NaGdF_4$:50%Nd,10%Yb (a2 – d2), and corresponding size distributions (a3 – d3) with different doping concentration of Tm^{3+} in core. a, 0.2%; b, 0.5%; c, 1%; d, 3%. Scale bars are 100 nm. (e) Typical XRD patterns of $NaGdF_4$:Yb,Tb,Tm and $NaGdF_4$:Yb,Tb,Tm@$NaGdF_4$:Nd,Yb nanoparticles. The XRD patterns show that as-prepared nanoparticles are hexagonal phased structure.

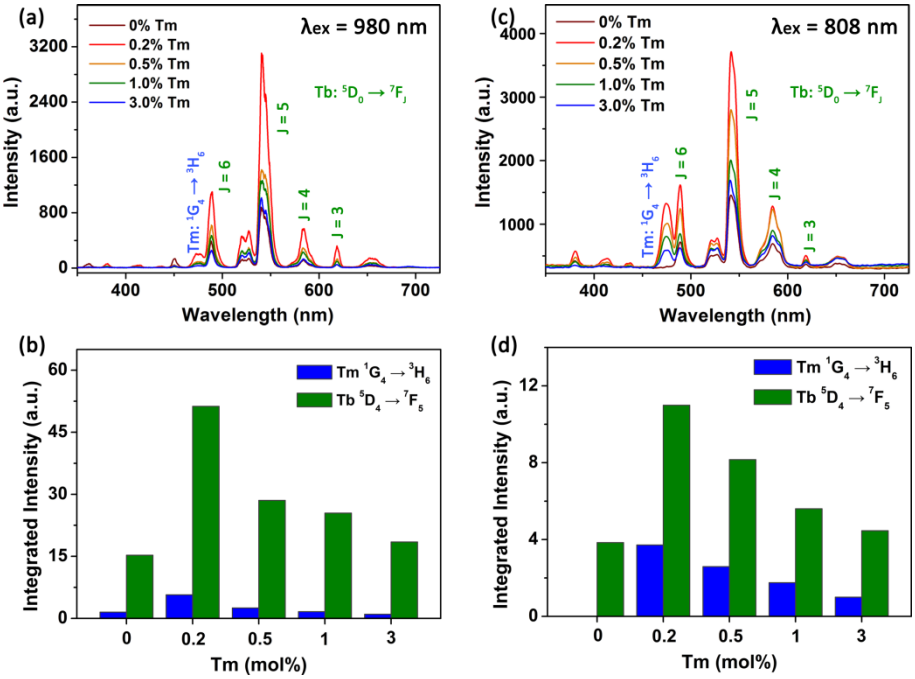

Figure S19. Multicolor upconversion emission spectra of $NaGdF_4$:30%Yb,10%Tb,Tm@$NaGdF_4$:50%Nd,10%Yb nanoparticles as a function of Tm^{3+} doping concentration (a, c) and corresponding integrated intensity (b, d). It is clear that typical 475 nm emissions ($^1G_4 \rightarrow {}^3H_6$) of Tm^{3+} are much stronger after doping with adequate amount of Tm^{3+}. And 0.2% Tm^{3+} is more adequate to produce multicolor emissions with Tb^{3+}.

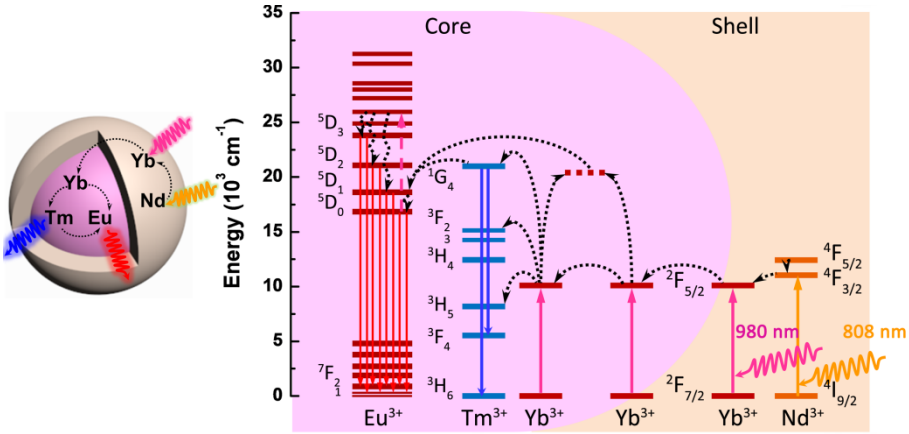

Scheme S4. Schematic design (left) and simplified energy transfer diagram of multicolor-emitting $NaGdF_4$:30%Yb,10%Eu,Tm@$NaGdF_4$:50%Nd,10%Yb nanoparticles under NIR excitation. Note that only partial energy levels of Nd^{3+}, Eu^{3+} and Tm^{3+} are shown for clarity.

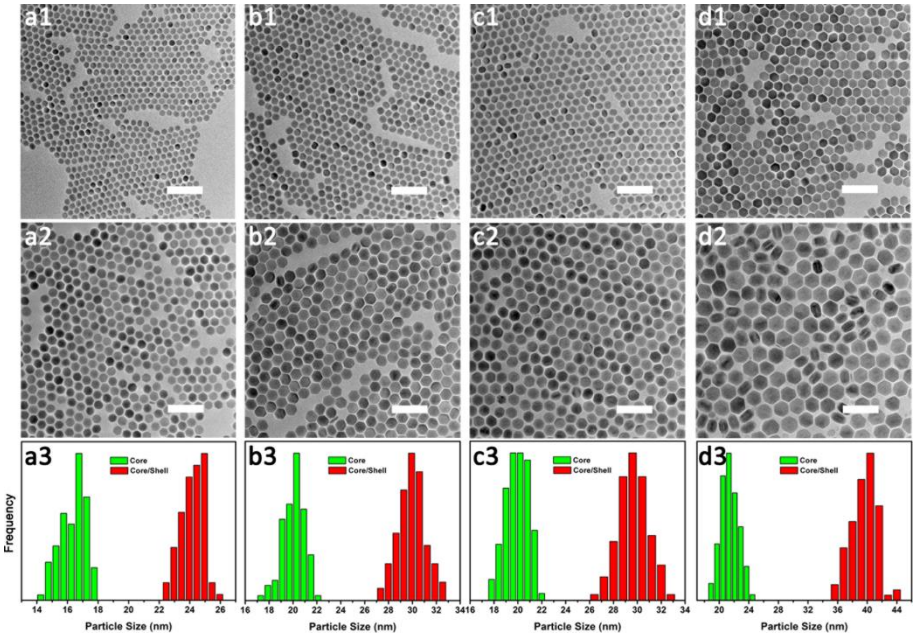

Figure S20. TEM images of $NaGdF_4$:30%Yb,10%Eu,Tm (a1 – d1), $NaGdF_4$:30%Yb,10%Eu,Tm@$NaGdF_4$:50%Nd,10%Yb (a2 – d2), and corresponding size distributions (a3 – d3) with different doping concentration of Tm^{3+} in core. a, 0.2%; b, 0.5%; c, 1%; d, 3%. Scale bars are 100 nm.

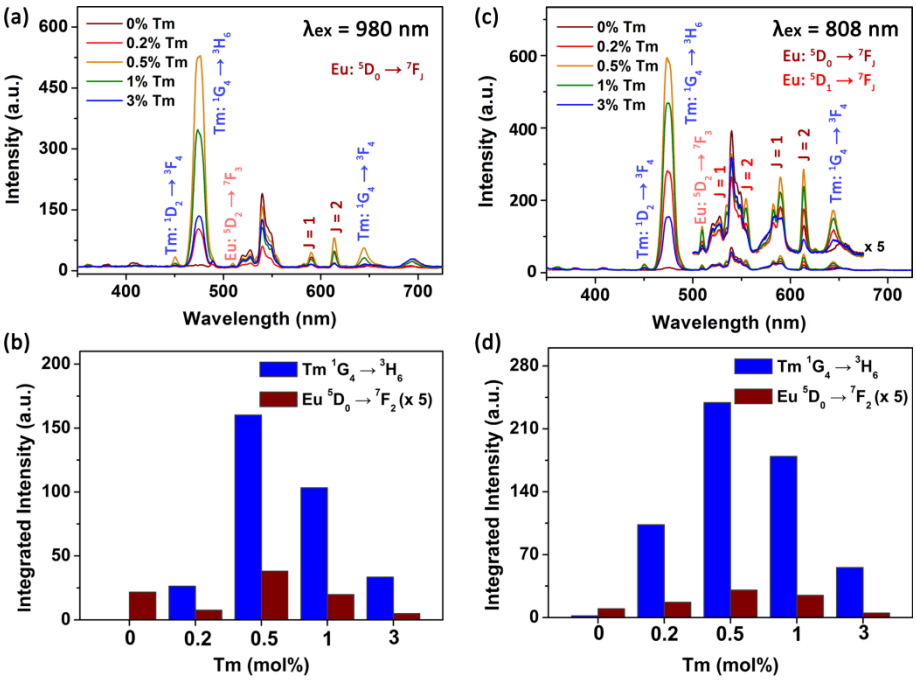

Figure S21. Multicolor upconversion emission spectra of $NaGdF_4$:30%Yb,10%Eu,Tm@$NaGdF_4$:50%Nd,10%Yb nanoparticles as a function of Tm^{3+} content (a, c) and corresponding integrated intensity (b, d). Typical 450 nm ($^1D_2 \rightarrow {}^3F_4$), 475 nm ($^1G_4 \rightarrow {}^3H_6$), and 645 nm ($^1G_4 \rightarrow {}^3F_4$) emissions of Tm^{3+} are much stronger with adequate amount of Tm^{3+}. Moreover, new Eu^{3+} emissions (510 nm, $^5D_2 \rightarrow {}^7F_3$; 535 nm, $^5D_1 \rightarrow {}^7F_1$ and 555 nm, $^5D_1 \rightarrow {}^7F_2$) appeared after co-doping with Tm^{3+} under 808 nm excitation. Thus 0.5% Tm^{3+} benefited to produce multicolor emissions with Eu^{3+}.

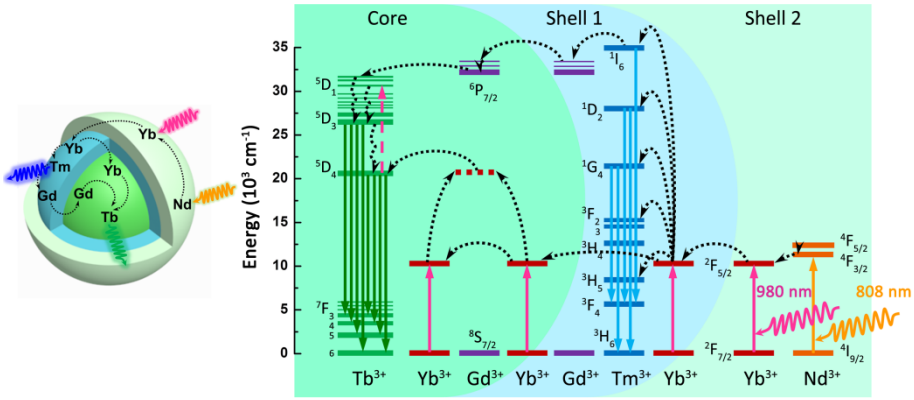

Scheme S5. Schematic design (left) and simplified energy transfer diagram of multicolor-emitting $NaGdF_4$:Yb,15%Tb@$NaGdF_4$:50%Yb,1%Tm@$NaYF_4$:50%Nd,10%Yb nanoparticles under NIR excitations (right). Note that only partial energy levels of Nd^{3+}, Gd^{3+}, Tb^{3+} and Tm^{3+} are shown for clarity.

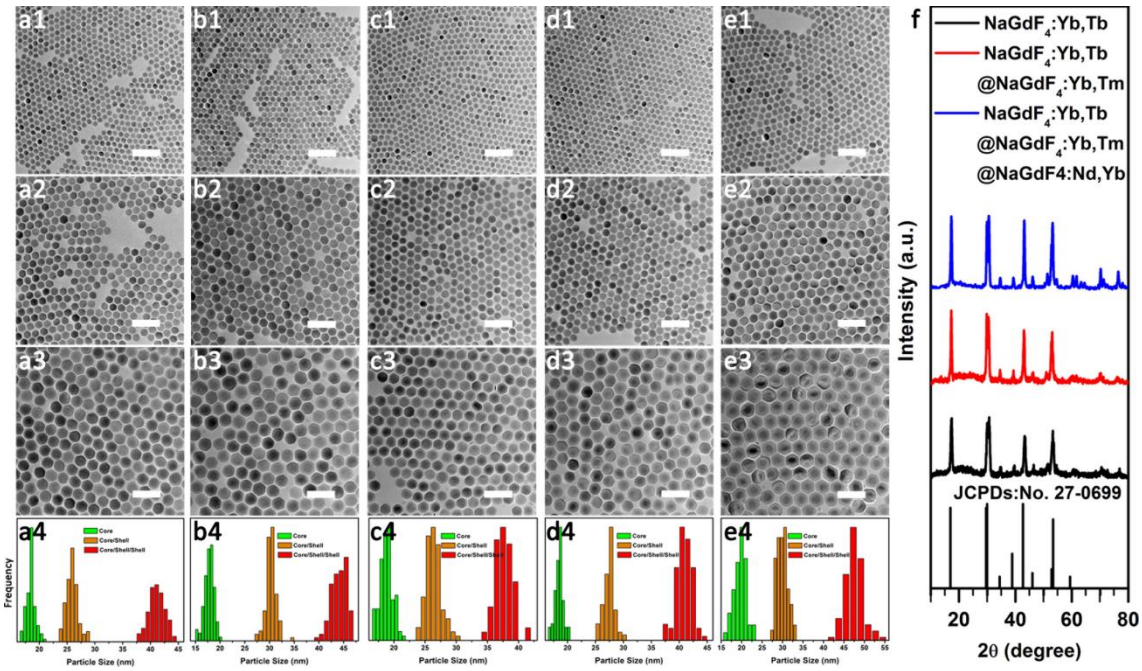

Figure S22. (a – e) TEM images of $NaGdF_4$:Yb,15%Tb (a1 – e1), $NaGdF_4$:Yb,15%Tb@$NaGdF_4$:50%Yb,1%Tm (a2 – e2), $NaGdF_4$:Yb,15%Tb@$NaGdF_4$:50%Yb,1%Tm@$NaYF_4$:50%Nd,10%Yb (a3 – e3), and corresponding size distributions (a4 – e4) with different doping concentration of Yb^{3+} in core. a, 0%; b, 10%; c, 20%; d, 30%; e, 40%. Scale bars are 100 nm. (f) Typical XRD patterns of $NaGdF_4$:Yb,Tb, $NaGdF_4$:Yb,Tb@$NaGdF_4$:Yb,Tm, and $NaGdF_4$:Yb,Tb@$NaGdF_4$:Yb,Tm@$NaYF_4$:Nd,Yb nanoparticles. The XRD patterns show that as-prepared nanoparticles are hexagonal phased structure.

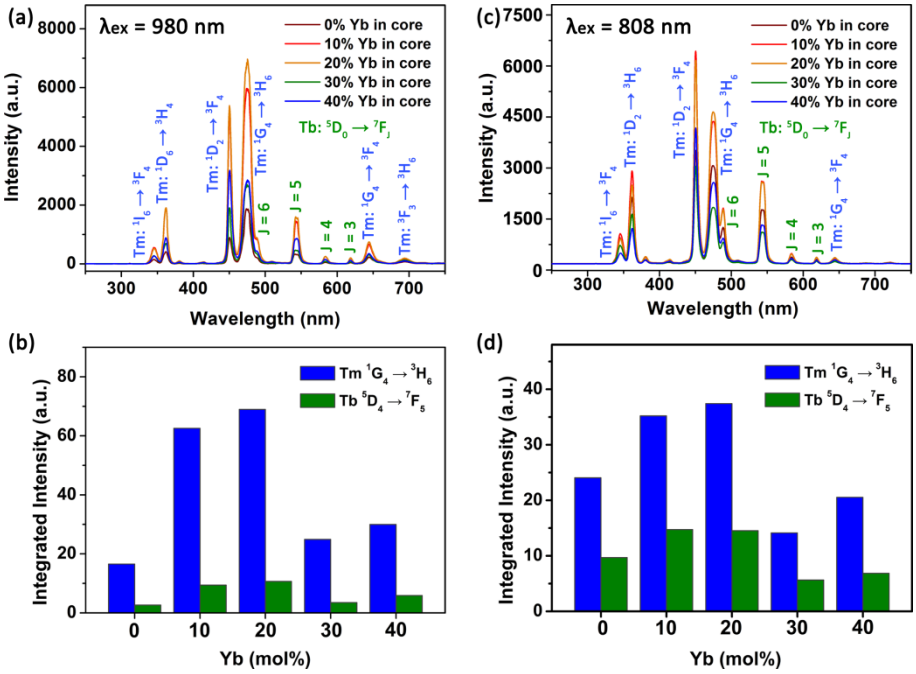

Figure S23. Multicolor upconversion emission spectra of $NaGdF_4$:Yb,15%Tb@$NaGdF_4$:50%Yb,1%Tm@$NaYF_4$:50%Nd,10%Yb nanoparticles as a function of Yb^{3+} centent in core (a, c) and corresponding integrated intensity (b, d). Typical emissions of both Tb^{3+} and Tm^{3+} are prominent in spectra.

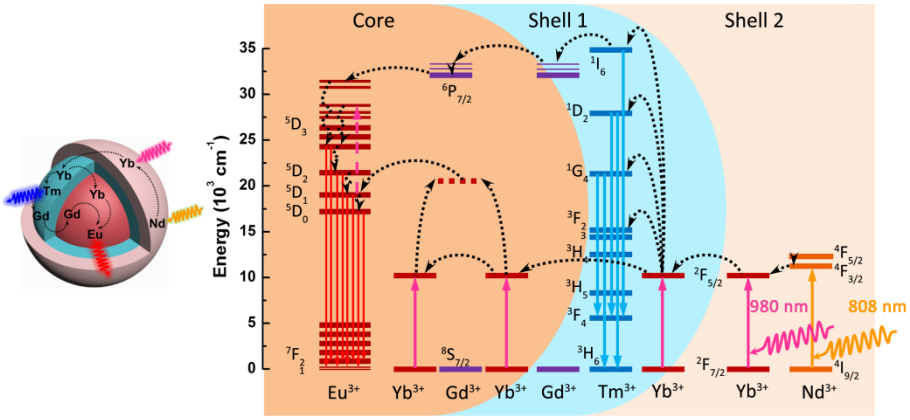

Scheme S6. Schematic design (left) and simplified energy transfer diagram of multicolor-emitting $NaGdF_4$:Yb,15%Eu@$NaGdF_4$:50%Yb,1%Tm@$NaYF_4$:50%Nd,10%Yb nanoparticles under NIR excitations (right). Note that only partial energy levels of Nd^{3+}, Gd^{3+}, Eu^{3+} and Tm^{3+} are shown for clarity.

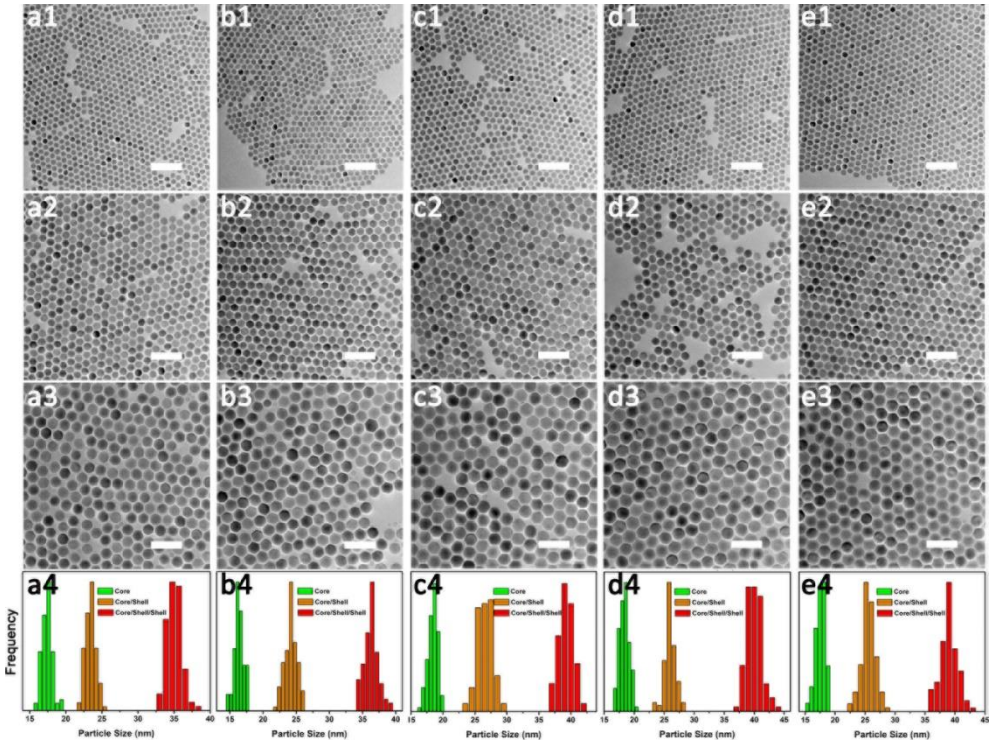

Figure S24. TEM images of $NaGdF_4$:Yb,15%Eu (a1 – e1), $NaGdF_4$:Yb,15%Eu@$NaGdF_4$:50%Yb,1%Tm (a2 – e2), $NaGdF_4$:Yb,15%Eu@$NaGdF_4$:50%Yb,1%Tm@$NaYF_4$:50%Nd,10%Yb (a3 – e3), and corresponding size distributions (a4 – e4) with different content Yb^{3+} in core. a, 0%; b, 10%; c, 20%; d, 30%; e, 40%. Scale bars are 100 nm.

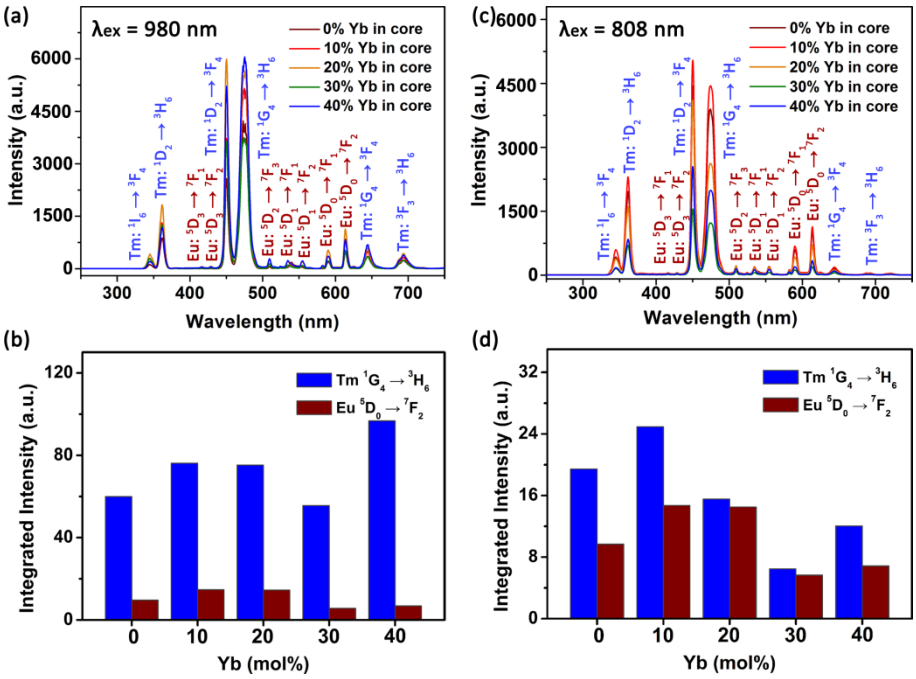

Figure S25. Multicolor upconversion emission spectra of $NaGdF_4$:Yb,15%Eu@$NaGdF_4$:50%Yb,1%Tm@$NaYF_4$:50%Nd,10%Yb nanoparticles as a function of Yb^{3+} content in core (a, c) and corresponding integrated intensity (b, d). Typical emissions of both Eu^{3+} and Tm^{3+} are prominent in spectra.

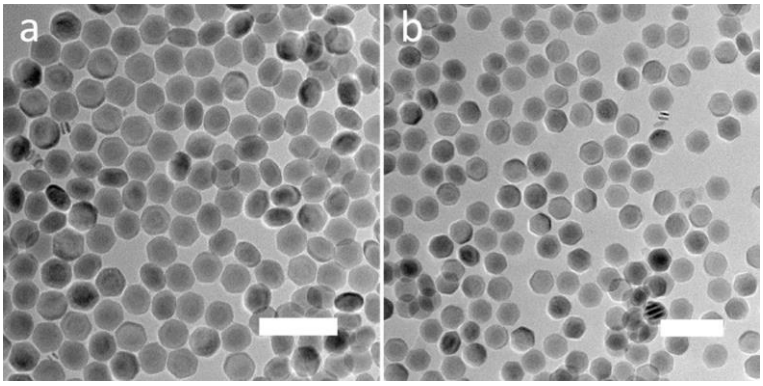

Figure S26. TEM images of hydrophilic PAA modified multicolor-emitting $NaGdF_4$: 20%Yb,15%Tb@$NaGdF_4$:50%Yb,1%Tm@$NaYF_4$:50%Nd,10%Yb (a) and $NaGdF_4$:20%Yb,15%Eu@$NaGdF_4$:50%Yb,1%Tm@$NaYF_4$:50%Nd,10%Yb (b) nanoparticles dispersed in deionized water. Scale bars are 100 nm.

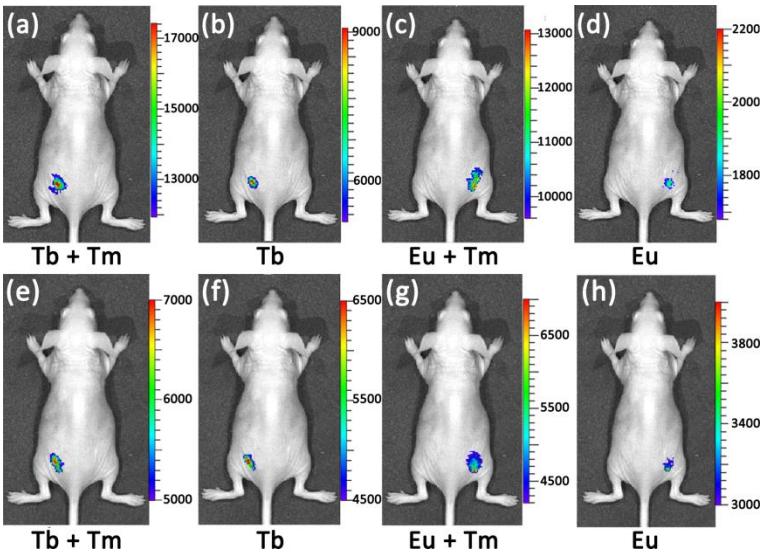

Figure S27. Multicolor *in vivo* imaging pictures of upconversion luminescence from Tb and Tm, Tb, Eu and Tm, and Eu under 980 nm (a – d) and 808 nm (e – h) excitation, respectively. The multicolor UCNPs were subcutaneously injected at the left and right back side of a mouse, respectvely.

References:

[S1] (a) H. X. Mai, Y. W. Zhang, R. Si, Z. G. Yan, L. D. Sun, L. P. You, C. H. Yan, *J. Am. Chem. Soc.* **2006**, *128*, 6426; (b) J.-C. Boyer, F. Vetrone, L. A. Cuccia, J. A. Capobianco, *J. Am. Chem. Soc.* **2006**, *128*, 7444; (c) H. X. Mai, Y. W. Zhang, L. D. Sun, C. H. Yan, *J. Phys. Chem. C* **2007**, *111*, 13721.

[S2] A. G. Dong, X. C.Ye, J. Chen, Y. J. Kang, T. Gordon, J. M. Kikkawa, C. B. Murray, *J. Am. Chem. Soc.* **2011**, *133*, 998